# ARMA systems in wind engineering

Yousun Li and A. Kareem

*Structural Aerodynamics and Ocean System Modeling Laboratory, Cullen College of Engineering, University of Houston, Houston, TX 77204-4791, USA*

The time domain solution of the equations of motion of structures subjected to a stochastic wind field is often obtained by a step-by-step integration approach. The loading is described by simulated time histories of the aerodynamic force. Recently, autoregressive and moving average (ARMA) recursive models have been utilized to simulate the time series of wind loads. Based on the system dynamic characteristics, the time-integration schemes require that the time increment should not exceed a prescribed value. This study focuses on the development of procedures to simulate realizations of wind loading with small time increments which are required by the time-integration schemes. An ARMA algorithm based on a three-stage-matching method and a scheme which combines ARMA and digital interpolation filters are presented to efficiently simulate realizations of wind loads at the prescribed time increments.

## INTRODUCTION

The time domain analysis of structures subjected to stochastic wind loading requires simulation of the discrete time histories of wind loading. The simulated time series are required to match single-point power spectral density functions and multiple-point correlation structures. Among the various simulation techniques, ARMA (autoregressive and moving average) modelling offers a computationally efficient scheme and requires minimum computer storage (e.g., Spanos and Mignolet[14]). A structure subjected to wind is generally discretized into a number of sections to describe wind loads effectively by taking into account the spatio-temporal characteristics of the wind velocity field. The correlated wind field at different sections is described by a multi-variate ARMA system. The coefficient matrices may be determined by the maximum entropy method (MEM). However, for the multi-variate ARMA models MEM requires solving a large number of nonlinear equations. Many other techniques have been developed to reduce this computational effort. A typical example is the two-stage-matching method for developing ARMA models (e.g., Samaras et al.[10] and Spanos and Schultz[13]). While most of the previous studies have focused on matching a univariate or a multivariate ARMA model to a prescribed spectral description of wind field, little attention has been paid to the requirement of time-integration schemes concerning the choice of the time increment. This requirement is primarily the time increment used in the integration scheme, which is often quite small to ensure that the energy content of the highest frequency component that is likely to excite the structure is accurately described. This paper focuses on the development of ARMA models for the wind field and its load effects with particular emphasis on the efficient simulation techniques to generate time series with small time steps.

## WIND FLUCTUATIONS AND LOAD EFFECTS

The wind velocity field is characterized by a multi-dimensional multi-variate random process. However, in the applications dealing with the digital simulation of wind field and its interaction with engineering structures the description of wind is often limited to the longitudinal field. This simplification is justified at this time due to a lack of quantitative models that describe the flow field in the separated flow regions. In the longitudinal direction, the quasi-steady and strip theories are successfully utilized to model wind. The longitudinal wind velocity at a location $r = (x, z)$ is described by a mean and a fluctuating component

$$U(t, r) = \bar{U}(z) + u(t, r) \tag{1}$$

The mean longitudinal wind velocity is described by a logarithmic law or a power law (Simiu and Scanlan[12]). The latter has been widely used in many design codes because of its simplicity.

In order to formulate the total fluctuating wind loading on a structure, it is necessary to formulate expressions for the single or multiple-point statistics of the wind velocity field. At the simplest level, a power spectral density represents the frequency content of wind fluctuations at any location. There are several descriptions of the power spectra available in the literature over a variety of terrains. In general, the spectral forms tend to agree in that they approach the Kolmogorov limit at high frequency, but all the spectra differ in their treatment of the low frequencies (Kareem[6]). The spectral descriptions due to Davenport[2] and Harris[3] are most commonly used for land-based structures, while for offshore applications spectrum due to Kareem[5] is more suitable. These spectra will be utilized to derive the ARMA models for the simulation of the wind field.

The next level of the wind velocity field description involves multiple-point statistics, i.e., the cross-spectral

density function, which is given by

$$G_u(\mathbf{r}, \mathbf{r}'; f) = \sqrt{(G_u(\mathbf{r}, f)G_u(\mathbf{r}', f))}\gamma(\mathbf{r}, \mathbf{r}'; f) \quad (2)$$

$$\gamma(\mathbf{r}, \mathbf{r}'; f) = \exp\left\{\frac{-f[C_h^2(x-x')^2 + C_v^2(z-z')^2]^{1/2}}{\frac{1}{2}[\bar{U}(z) + \bar{U}(z')]}\right\} \quad (3)$$

where $C_h$ and $C_v$ are generally equal to 10 and 16, respectively (Davenport[2]).

The wind load effects on structures can be simulated either by generating a space–time structure of the wind field or by directly generating fluctuating loads induced by wind fluctuations. In the first approach the wind velocity fluctuations are simulated at the centroid of various sections of the discretized structure. The wind is assumed to be fully correlated on each section and the corresponding wind force on the $i$th section is given by

$$F_i = 0.5\rho A_i C_d[U_i(t) - \dot{D}_i(t)]^2 \quad (4)$$

in which $\rho$, $A_i$, $C_a$ denote air density, the $i$th sectional area and drag coefficient, respectively, $U_i(t)$ denotes wind velocity at the centroid of the $i$th section, and $\dot{D}_i(t)$ is the structural velocity. The assumption of full-correlation of wind velocity field on each section may overestimate the total wind load. However, for compliant offshore structures, e.g., tension leg platform (Li[7]), the low frequency parts of the fluctuating wind field are of interest which are nearly fully-correlated over a small section.

Alternatively, the fluctuating wind force may be directly estimated by ignoring the quadratic and the structural velocity terms in the previous equations. In this formulation, the integration of wind force expressed over a section incorporates the lack of correlation (Davenport[2] and Kareem[5]). The power spectral density of the wind force acting on the $i$th section and the cross-spectral density function between the $i$th and $j$th wind forces are expressed as

$$G_{F_{ii}}(f) = 4\rho^2 C_d^2 \bar{U}_i^2 G_{u_{ii}}(f)L(f) \quad (5)$$

and

$$G_{F_{ij}}(f) = \sqrt{G_{F_{ii}}(f)G_{F_{jj}}(f)}\gamma_{ij}(f) \quad (6)$$

in which $G_{u_{ii}}(f)$ is the spectral density function of wind fluctuation and $\gamma_{ij}(f)$ is defined in equation (3), and

$$L(f) = \frac{4}{(\gamma_x\gamma_z C_x C_z)^2}[\exp(-\gamma_x C_x) + \gamma_x C_x - 1]$$
$$\times [\exp(-\gamma_z C_z) + \gamma_z C_z - 1] \quad (7)$$

where

$$\gamma_z = \frac{2f\phi D}{\bar{U}_i}; \qquad \gamma_x = \frac{2f\phi B}{\bar{U}_i}; \qquad \phi = \frac{\sqrt{1 + \left(\frac{C_x B}{C_z D}\right)^2}}{\left(1 + \frac{C_x B}{C_z D}\right)}$$

in which $B$ and $D$ are the width and height of a section. In this approach, a vector of time series of wind loading, $F(n\,\Delta t)$ is directly generated by a multi-variate ARMA model matched to the wind force spectral description.

## ARMA MODELLING

An ARMA model of orders $P$ and $Q$ is defined as a linear filter that permits simulation of the wind velocity or force $y(\Delta t)$ (of order $M$) by its past time histories and the past and present white noise processes:

$$y(n\,\Delta t) + \sum_{r=1}^{P} \mathbf{A}_r y[n-r]\,\Delta t] = \sum_{r=0}^{Q} \mathbf{B}_r \varepsilon_{n-r} \quad (8)$$

in which $\mathbf{A}_r$ and $\mathbf{B}_r$ are AR and MA coefficient matrices, and $\varepsilon_{n-r}$ is a vector containing white noise with a zero mean and a unit variance. The coefficient matrices are determined from the specified spectral description of the random field to be simulated. A desirable feature of ARMA modelling is that the model orders and the error are small, since the total order translates into the number of multiplications and additions at each discrete time interval during the simulation procedure.

The transfer function of an ARMA model is given by

$$\hat{\mathbf{H}}(f) = \left[\mathbf{I} + \sum_{r=1}^{P} \mathbf{A}_r \exp(-2\pi f r\,\Delta t)\right]^{-1}$$
$$\times \left[\sum_{r=0}^{Q} \mathbf{B}_r \exp(-2\pi f r\,\Delta t)\right] \quad (9)$$

Accordingly, the spectral density function is expressed as

$$\hat{\mathbf{G}}(f) = 2\hat{\mathbf{H}}(f)\hat{\mathbf{H}}^*(f)\,\Delta t \quad (10)$$

in which $*$ denotes complex conjugation.

The model error can be defined as

$$e_{ij} = \frac{\int_0^{f_n} |\hat{G}_{ij}(f) - G_{ij}(f)|\,df}{\int_0^{f_n} |G_{ij}(f)|\,df} \quad (11)$$

where $f_n$ is the Nyquist frequency.

The transfer functions of ARMA models are characterized by zeros and poles. The versatility of an ARMA process is demonstrated by the fact that a stationary time series can often be described by an ARMA model involving fewer parameters than an MA or AR process individually. A low-order ARMA model could produce a small error if the coefficients are suitably selected. The application of the maximum entropy method to determine the coefficient matrices of a multivariate ARMA model requires the solution of a large number of nonlinear equations. Therefore, alternative techniques have been developed to circumvent this difficulty. One of these approaches is the two-stage-matching method, by which an ARMA model is developed based on a prior AR model. There are a number of different approaches to the two-stage-matching method, e.g. Samaras et al.[10] and Spanos and Shultz[13].

The basic concept involves an AR model with order $P'$ that is first matched to the covariance matrices $\mathbf{C}_{yy}(r\,\Delta t)$ $(r = 0, 1, \ldots, P')$. Then the covariance functions between $y(n\,\Delta t)$ and $\varepsilon_n$, $\mathbf{C}_{y\varepsilon}(m\,\Delta t)$, are obtained by the AR model,

$$\mathbf{C}_{y\varepsilon}(m\,\Delta t) = 0 \qquad \text{for } m > 0$$
$$\mathbf{C}_{y\varepsilon}(m\,\Delta t) = \mathbf{B}_0' \qquad \text{for } m = 0$$

and

$$C_{y\varepsilon}(m\,\Delta t) = -\sum_{r=1}^{m} A_r C_{yy}^T[(r+m)\,\Delta t] \qquad \text{for } m<0 \quad (12)$$

The ARMA model of order $P$ and $Q$ is formulated by matching a given $C_{yy}(r\,\Delta t)$ and $C_{y\varepsilon}(m\,\Delta t)$ obtained from the AR model, e.g., Auto/Cross-Correlation Matching Procedure,

$$C_{y\varepsilon}(-m\,\Delta t) + \sum_{r=1}^{\min(m,P)} A_r C_{y\varepsilon}[(r-m)\,\Delta t] = B_m \quad (13)$$

and

$$C_{yy}(-m\,\Delta t) + \sum_{r=1}^{P} A_r C_{yy}[(r-m)\,\Delta t] = \sum_{r=1}^{Q} B_r C_{y\varepsilon}^T[(m-r)\,\Delta t]$$
$$(14)$$
$$(m=0,1,2,\ldots,Q)$$

However, for some target spectral descriptions straightforward evaluation of the initial AR model poses difficulties. Alternatively, the derivation of ARMA models may be based on a moving average (MA) linear system which does not introduce the difficulties experienced in the previous approach (Spanos and Mignolet[14]). In this manner, an ARMA model can be formulated by the solution of a number of linear equations. Computationally, this procedure is very convenient (Spanos and Mignolet[14]).

In the two-stage matching method involving the initial AR model, the ARMA model coefficients with given $P$ and $Q$ are not unique, since they depend on the prior AR order $P'$. There are three parameters to be selected: $P'$, $P$, and $Q$ and the time increment $\Delta t$. Samaras et al.[10] used the following relationship between these parameters,

$$P=Q \quad \text{and} \quad P' \geqslant P+Q+2 \quad (15)$$

Optimal model orders may only be obtained from a larger number of combinations of the above parameters. In the present study, an interactive computer algorithm was developed to study the effects of various combinations of the parameters on the model accuracy. The model errors in terms of $P'$, $P$, $Q$ and $\Delta t$ were evaluated by means of an example of fluctuating wind velocities at two locations ($x=0$, $z_1=300$ ft and $z_2=60$ ft) described by the Harris and Davenport wind spectra. Figures 1(a) and (b) illustrate the effect of $P'$ on the model error for given values of $P+Q$ and $\Delta t$. In these figures $G_{11}$ and $G_{12}$ denote the spectral density function of the wind velocity at section 1 and cross-spectral density function between velocities at sections 1 and 2, respectively. It is noted in these figures that an increase in $P'$ is generally favourable to the model accuracy. Since $P'$ does not appear in the time simulation procedure, a large value of $P'$ may not influence the final simulation scheme. On the other hand, a large value of $P'$ could require very extensive computational effort in the initial development of the ARMA model. An empirical relation based on the present study suggests

$$P' = 3(P+Q) \quad (16)$$

One further remark is appropriate here. For a fixed $P+Q$, a selection of $P$ and $Q$ can affect the model error, as shown in Fig. 2. For the wind field, it is recommended based on this
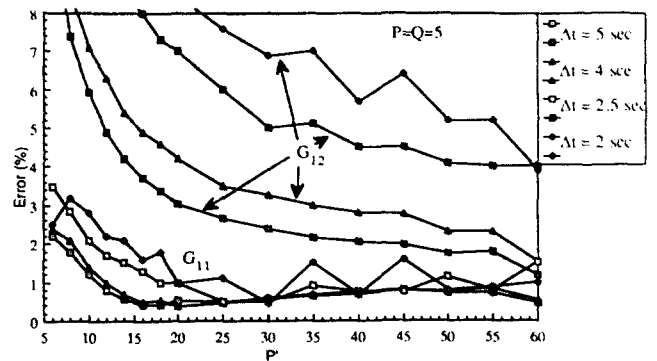


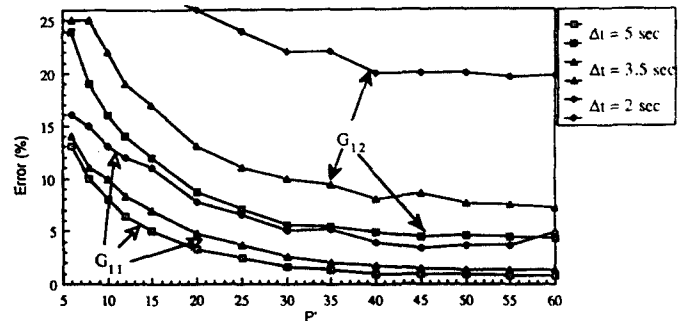Fig. 1(a). Error in terms prior-AR order (Harris spectrum)



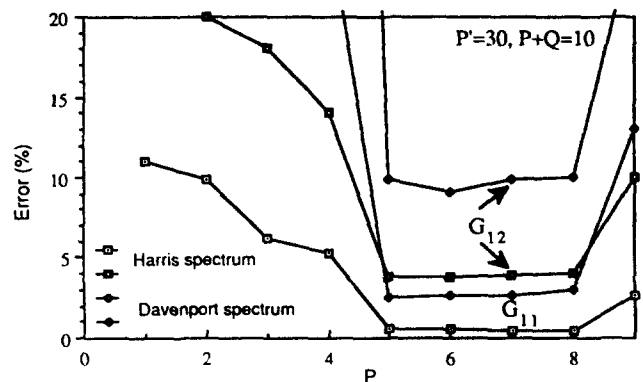Fig. 1(b). Error in terms of prior-AR order (Davenport spectrum)



Fig. 2. Error in terms of AR order

study to use

$$P \geqslant Q \quad (17)$$

Additionally, the time increment, $\Delta t$, also influences the model error. Approximately, the ARMA model involves a window of time period $(P+Q)\,\Delta t$. A decrease in $\Delta t$ could increase the model errors, as shown in Figs 1(a) and (b). It is also noted in Figs 1(a), (b) and Fig. 2 that the shape of the wind spectral density function can significantly affect the model accuracy. For example, an ARMA model used to match the wind spectrum with a finite value at zero frequency, such as the Harris spectrum, has higher accuracy than an ARMA model for the wind spectrum with a zero value at the zero frequency, such as the Davenport spectrum. It is important to note that the ARMA matching is also sensitive to the accuracy of the correlation functions derived from the given spectral density functions.

Typical examples of the comparisons between the target spectra and the estimated spectra are shown in Fig. 3, and the comparisons of the coherence functions are shown in

Fig. 4. It is noted that an ARMA model can be matched to the Harris wind spectrum with almost no discernible error in the entire frequency range. The difficulty in matching the Davenport wind spectrum is primarily due to the representation of the sharp drop in the spectral ordinates near the zero frequency.

In most of the above examples, the time series were simulated for large $\Delta t$ ($\geq 2$ sec), in which the spectral density of the wind velocity at the Nyquist frequency still has significant energy. However, it is generally required to have a much smaller $\Delta t$ due to the following reasons: (1) The natural frequency of the highest mode of interest may be high; (2) The structure may be subjected to other environmental loads, such as wave loads, earthquakes, etc.,
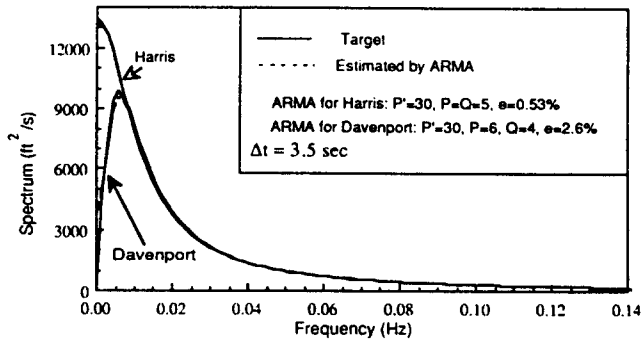


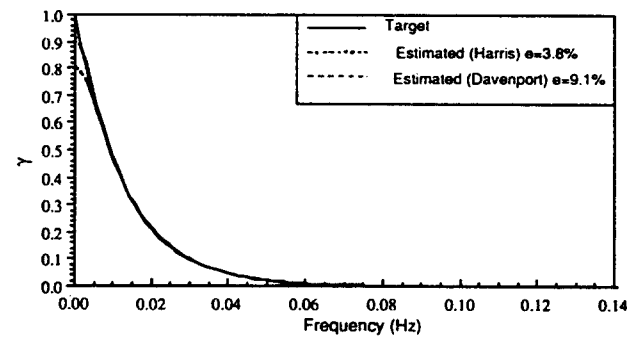*Fig. 3. Comparisons of wind spectra density functions*



*Fig. 4. Coherence function*

which have high frequencies, hence, the time series of wind loads must have a small time increment to be consistent with the time series of other loads; (3) Depending on the numerical scheme, the accuracy and stability during the time-integration procedure may require that the time increment does not exceed a prescribed maximum value. If the required time increment is 0.5 sec, then the Nyquist frequency would be 1 Hz, but generally a significant portion of wind energy is less than 0.1 Hz. Also the coherence function is often significant only within a small portion of the entire frequency range. Therefore, it becomes quite difficult to match an ARMA model to wind fields with small $\Delta t$. In the following sections, the discussion focuses on two methodologies developed in this study to alleviate such difficulties: a three-stage-matching method and interpolation models.

## THREE-STAGE MATCHING METHOD

A three-stage-matching method is proposed that involves the introduction of a suitable parameter $\alpha$ which transforms the target process $y(\Delta nt)$ into $z(n \Delta t)$

$$z(n \Delta t) = y(n \Delta t) - \alpha y[(n-1) \Delta t] \tag{18}$$

Utilizing the backshift operator $B$, the preceding equation reduces to

$$z(n \Delta t) = (1 - \alpha B) y(n \Delta t) \tag{19}$$

The $(i,j)$th element of the spectral density matrix of $z(t)$ becomes

$$G_{z_{ij}}(f) = [1 + \alpha^2 - 2 \cos(2\pi f \Delta t)]^2 G_{y_{ij}}(f) \tag{20}$$

If $\alpha = 1$, then equation (19) is similar to the seasonal difference method in the Box–Jenkins approach (Box and Jenkins[1]). However, $\alpha = 1$ leads to a zero spectral ordinate in equation (20), and it is not invertible. Hence, $\alpha$ is selected such that $0 < \alpha < 1$ which ensures a slow decrease in the spectral ordinates of $z(n \Delta t)$ with an increase in frequency. For the Harris wind spectrum, it is recommended to use $\alpha = 0.94 \sim 0.98$.

*Table 1. Wind and wind loading conditions*

**WIND PARAMETERS**

| | |
|---|---|
| Spectrum | Harris |
| Mean wind velocity at 32.8 ft high | 29.84 ft/sec |
| Power exponent | 0.34 |
| Length scale | 4000 ft |
| Wind surface stress coefficient | 0.05 |
| Decay Parameter (horizontal and vertical) | 10, 16 |
| Air density | 0.0019 Slug/ft³ |

**WIND DATA ON EACH SECTION**

| No. | z (ft) | U (ft/s) | $C_u$ (ft²/s²) | | | | |
|---|---|---|---|---|---|---|---|
| 1 | 540 | 77.34 | 287.1 | 168.2 | 125.6 | 98.17 | 76.01 |
| 2 | 420 | 71.01 | 168.2 | 287.1 | 162.7 | 118.4 | 87.74 |
| 3 | 300 | 63.33 | 125.6 | 162.7 | 287.1 | 154.8 | 105.9 |
| 4 | 180 | 52.23 | 98.17 | 118.4 | 154.8 | 287.1 | 144.9 |
| 5 | 60 | 36.64 | 76.01 | 87.74 | 105.9 | 144.9 | 287.1 |

**WIND FORCE DATA ON EACH SECTION**

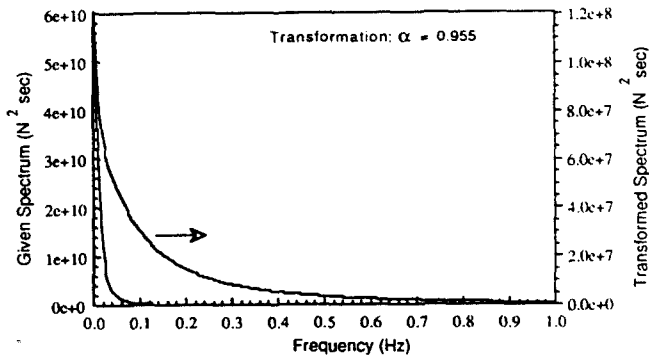| No. | $C_d$ | W (ft) | H (ft) | Mean (kN) | $C_F$ kN²) | | | |
|---|---|---|---|---|---|---|---|---|
| 1 | 1.2 | 100 | 120 | 81.83 | 855.8 | 566.2 | 394.9 | 265.6 | 142.5 |
| 2 | 1.2 | 100 | 120 | 68.98 | 566.2 | 705.8 | 444.3 | 284.6 | 147.5 |
| 3 | 1.2 | 100 | 120 | 54.87 | 394.9 | 444.3 | 544.6 | 312.2 | 153.0 |
| 4 | 1.2 | 100 | 120 | 38.77 | 265.6 | 284.6 | 312.2 | 373.3 | 170.6 |
| 5 | 1.2 | 100 | 120 | 18.37 | 142.5 | 147.5 | 153.0 | 170.6 | 158.3 |

Fig. 5. Spectra before and after pre-transformation

An example of wind loads acting on a tall building with the lowest natural frequency equal to 0.2 Hz (the wind and the wind force data are listed in Table 1) is used to illustrate this approach. The building face is divided into five segments. It is required to have the wind load simulated at an interval of at least 0.5 sec. Figure 5 demonstrates the spectral densities of the wind loads at the 5th level before and after the transformation given in equation (18) with $\alpha = 0.955$. It is noted in this figure that the wind load spectral ordinates are negligible within the frequency range $0.1 \sim 1$ Hz. However, after the transformation, the spectrum covers the entire frequency range up to the Nyquist frequency and decays slowly with the frequency.

$z(n \, \Delta t)$ can be matched by an ARMA model utilizing the two-stage-matching procedure discussed in the preceding section,

$$z(n \, \Delta t) + \sum_{r=1}^{pz} A_r^z z[(n-r) \, \Delta t] = \sum_{r=0}^{Q} B_r \varepsilon_{n-r} \qquad (21)$$

which, after substitution in equation (19), takes the form of equation (8), in which

$$P = P^z + 1 \qquad (22)$$

and

$$A_1 = A_1^z - \begin{bmatrix} \alpha & 0 & \cdots & 0 \\ 0 & \alpha & \cdots & 0 \\ \vdots & \vdots & \cdots & 0 \\ 0 & \cdots & \cdots & \alpha \end{bmatrix} \qquad (23)$$

$$A_r = A_r^z - \alpha A_{r-1}^z \qquad \text{for } r > 1 \qquad (24)$$

In this example, an ARMA (4, 4) model from a prior AR (30) model has been matched for $z(n \, \Delta t)$. Subsequently, ARMA model (5, 4) for $y(n \, \Delta t)$ is formulated. The spectral density and the coherence functions of the target wind loads and those represented by the ARMA model are plotted in Fig. 6(a), (b), (c) and Fig. 7, and the errors are listed in Table 2. For convenience the frequency range is divided into $0 \sim 0.1$ Hz, $0.1 \sim 0.45$ Hz and $0.45 \sim 1$ Hz, in which different coordinate resolutions are used (Fig. 6(a), (b) and (c)). The input coherence function is negligible for $f > 0.1$ Hz, so Table 2 only provides the spectral and cross-spectral density errors below 0.1 Hz, and spectral density errors beyond 0.1 Hz. These figures and the table demonstrate the closeness between the target and estimated spectral functions, especially at high frequencies. However, there are some discrepancies in the cross-spectral density function for the
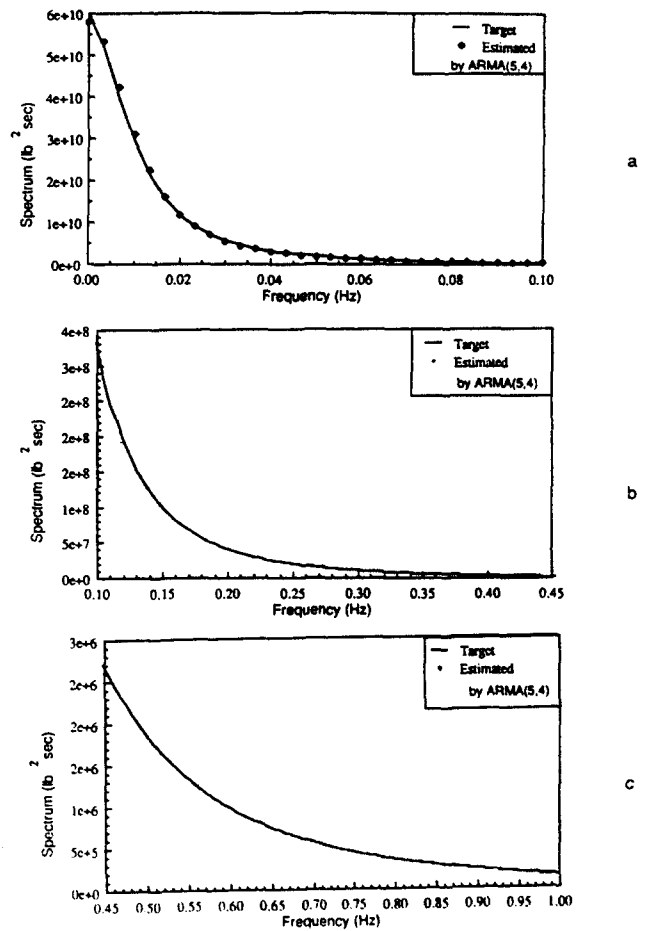


Fig. 6. Target and estimated wind load spectra on the 5th floor level. (a) 0.0–0.1 Hz; (b) 0.1–0.45 Hz; (c) 0.45–1.0 Hz
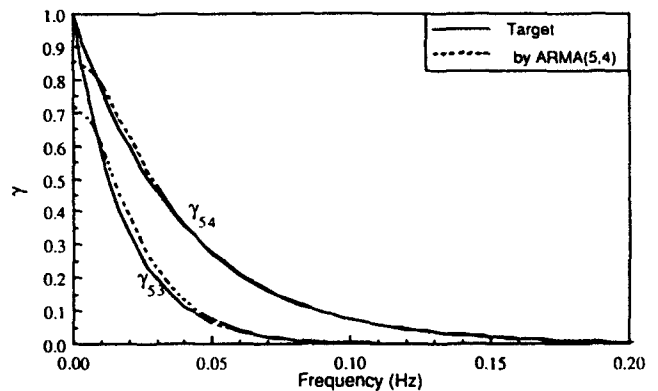


Fig. 7. Target and estimated coherence functions

Table 2. Errors in ARMA (5,4) by three-stage matching method

Error in matrix of spectral and cross-spectral density terms (in the frequency range less than 0.1 Hz)

| | | | | |
|---|---|---|---|---|
| **4%** | 10% | 22% | 36% | 57% |
| 10% | **4%** | 12% | 25% | 47% |
| 22% | 12% | **5%** | 14% | 34% |
| 36% | 25% | 14% | **5%** | 20% |
| 57% | 47% | 34% | 20% | **8%** |

Errors in spectral density functions (in the frequency range $0.1 \sim 1.0$ Hz)

| | | | | |
|---|---|---|---|---|
| **0.77%** | **0.84%** | **0.9%** | **1.5%** | **0.74%** |

Table 3. ARMA (5,4) parameters from the three-stage matching method

| | | | | | |
|---|---|---|---|---|---|
| AR 1: | -1.861E+00 | 1.567E-02 | 8.654E-02 | 5.829E-02 | -9.774E-02 |
| | 3.506E-02 | -1.945E+00 | -5.626E-03 | 3.056E-02 | -7.826E-02 |
| | 5.986E-02 | 2.425E-03 | -2.018E+00 | -6.049E-02 | -1.817E-02 |
| | 1.962E-02 | 1.142E-02 | -3.216E-02 | -2.046E+00 | 3.362E-02 |
| | -1.194E-01 | -1.116E-01 | -3.511E-02 | 1.626E-01 | -9.064E-01 |
| AR 2: | 3.408E-01 | -5.021E-01 | -1.454E-01 | -1.273E-01 | 5.610E-02 |
| | -5.657E-02 | 4.977E-01 | -1.129E-02 | -6.951E-02 | 4.171E-02 |
| | -8.566E-02 | -1.485E-02 | 5.923E-01 | 7.397E-02 | -3.346E-03 |
| | -3.574E-02 | -2.314E-02 | 3.919E-02 | 6.159E-01 | -3.811E-02 |
| | 1.463E-01 | 1.437E-01 | 2.691E-02 | -2.744E-01 | -9.627E-01 |
| AR 3: | 1.037E+00 | 4.606E-02 | 2.415E-02 | 5.706E-02 | 7.461E-02 |
| | 1.736E-02 | 9.835E-01 | 3.286E-02 | 3.630E-02 | 6.252E-02 |
| | -7.594E-04 | 1.907E-02 | 1.006E+00 | 3.036E-02 | 2.743E-02 |
| | 9.173E-03 | 9.556E-03 | 1.616E-02 | 1.033E+00 | -6.762E-03 |
| | 3.923E-02 | 3.686E-02 | 3.704E-02 | 3.642E-02 | 5.578E-01 |
| AR 4: | -5.641E-01 | -1.126E-02 | 5.298E-02 | 3.113E-02 | 4.929E-04 |
| | 6.292E-03 | -6.028E-01 | -1.956E-02 | 1.166E-02 | 2.109E-03 |
| | 3.735E-02 | -7.907E-03 | -6.603E-01 | -6.065E-02 | 5.562E-03 |
| | 1.213E-02 | 4.995E-03 | -3.210E-02 | -6.484E-01 | 4.069E-03 |
| | -8.558E-02 | -9.055E-02 | -3.232E-02 | 1.187E-01 | 6.625E-01 |
| AR 5: | 4.998E-02 | -5.613E-04 | -1.874E-02 | -1.942E-02 | -3.608E-02 |
| | -1.732E-03 | 6.871E-02 | 3.224E-03 | -9.120E-03 | -3.026E-02 |
| | -1.016E-02 | 1.080E-03 | 8.152E-02 | 1.612E-02 | -1.230E-02 |
| | -5.147E-03 | -2.830E-03 | 8.528E-03 | 8.296E-02 | 7.507E-03 |
| | 1.786E-02 | 2.051E-02 | 2.852E-03 | -4.282E-02 | -3.433E-01 |
| MA 0: | 2.059E+03 | 0.000E+00 | 0.000E+00 | 0.000E+00 | 0.000E+00 |
| | 7.329E+01 | 1.751E+03 | 0.000E+00 | 0.000E+00 | 0.000E+00 |
| | 1.657E+01 | 4.978E+01 | 1.419E+03 | 0.000E+00 | 0.000E+00 |
| | 5.622E+00 | 9.280E+00 | 3.121E+01 | 1.029E+03 | 0.000E+00 |
| | 1.986E+00 | 2.349E+00 | 4.274E+00 | 1.339E+01 | 5.461E+02 |
| MA 1: | -3.808E+01 | 1.167E+02 | 1.471E+02 | 6.942E+01 | -4.629E+01 |
| | 1.380E+02 | -1.723E+02 | 5.491E+01 | 4.589E+01 | -3.521E+01 |
| | 1.383E+02 | 4.528E+01 | -2.102E+02 | -1.894E+01 | 1.124E+00 |
| | 4.603E+01 | 2.678E+01 | -1.857E+01 | -1.464E+02 | 4.407E+01 |
| | -2.498E+02 | -1.911E+02 | -3.619E+01 | 1.928E+02 | 5.074E+02 |
| MA 2: | -1.687E+03 | 4.780E+01 | 4.962E+01 | -4.818E+00 | -5.726E+01 |
| | 1.950E+01 | -1.430E+03 | 2.448E+01 | 1.153E+00 | -4.713E+01 |
| | 5.141E+01 | -1.594E+01 | -1.202E+03 | -6.039E+00 | -1.083E+01 |
| | 1.389E+00 | -3.534E+00 | -2.933E+01 | -8.825E+02 | 3.502E+01 |
| | -1.605E+02 | -1.169E+02 | -5.054E+01 | 5.421E+01 | -8.957E+01 |
| MA 3: | -5.044E+01 | -1.186E+01 | -5.798E+01 | -4.161E+01 | -2.986E+01 |
| | -1.442E+01 | 2.726E+01 | -1.607E-01 | -2.288E+01 | -2.646E+01 |
| | -4.623E+01 | -8.831E-01 | 4.845E+01 | 2.366E+01 | -1.305E+01 |
| | -2.473E+01 | -1.168E+01 | 2.045E+01 | 2.546E+01 | 3.016E+00 |
| | 7.154E+01 | 6.920E+01 | 1.088E+00 | -8.873E+01 | -3.137E+02 |
| MA 4: | 1.388E+02 | -1.754E-01 | -1.366E+01 | -5.457E+00 | 3.182E-01 |
| | 6.956E+01 | 1.251E+02 | 1.200E+00 | -2.963E+00 | -3.071E-01 |
| | -1.229E-01 | 3.641E+00 | 1.112E+02 | 7.163E+00 | -1.914E+00 |
| | -4.173E+00 | -1.182E+00 | 8.053E+00 | 8.039E+01 | -3.280E+00 |
| | 2.856E+01 | 2.628E+01 | 6.430E+00 | -2.047E+01 | -4.471E+01 |
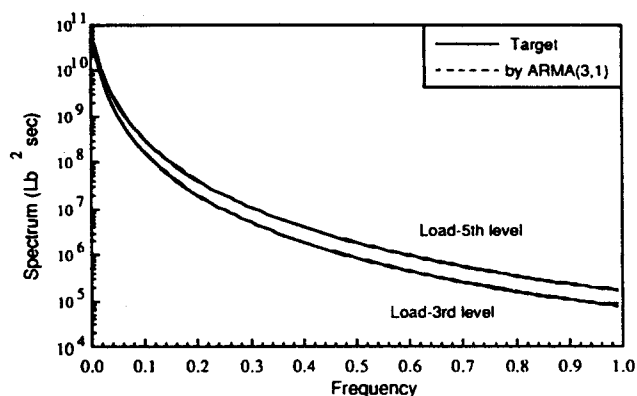


Fig. 8. Target and estimated spectra of wind loads

largely spaced points with low correlation. The parameters of the ARMA (5,4) model are listed in Table 3.

The ARMA model formulated by the three-stage-matching method is especially suitable for the representation of the high frequency spectra. If the low frequency wind loads are not important, it is possible to obtain a very low order ARMA model, e.g., ARMA (3, 1) for the above example (Fig. 8). The ARMA (3, 1) parameters are given in Table 4. The three-stage matching method involves selecting the parameter $\alpha$ in addition to $P'$, $P$ and $Q$. However, it does modify the shape of the spectral density functions which facilitates a convenient modelling, but it cannot modify the shape of the coherence function. This would result in some error in the cross-spectral density function, which is particularly amplified for largely spaced locations which generally exhibit a low level of correlation (Table 2). This method can be applied to most of the wind spectra, such as the Harris or Kareem spectra (Kareem[6]). For some wind spectra, such as the Davenport spectrum, which has a zero ordinate at the zero frequency, this method is not suitable.

## INTERPOLATION MODELS

A more general method to simulate time series of wind field involves a combination of an ARMA model and an interpolation model. Let the time increment in the ARMA

Table 4. ARMA (3, 1) parameters

| AR 1: | -1.352E+00 | 7.275E-02 | -2.921E-02 | -7.118E-02 | -4.768E-01 |
|---|---|---|---|---|---|
| | 5.600E-02 | -1.429E+00 | 4.438E-02 | -5.852E-02 | -4.940E-01 |
| | -1.360E-02 | 2.944E-02 | -1.425E+00 | 2.486E-02 | -4.381E-01 |
| | -1.759E-02 | -1.993E-02 | 1.466E-02 | -1.421E+00 | -9.103E-02 |
| | -6.720E-03 | -9.808E-03 | -1.237E-02 | 6.504E-04 | -1.568E+00 |
| AR 2: | 2.026E-01 | -2.060E-01 | 1.218E-02 | 1.017E-01 | 8.039E-01 |
| | -1.535E-01 | 3.250E-01 | -1.501E-01 | 6.933E-02 | 8.331E-01 |
| | 4.814E-03 | -9.851E-02 | 2.981E-01 | -1.158E-01 | 7.182E-01 |
| | 2.318E-02 | 2.154E-02 | -6.489E-02 | 2.555E-01 | 5.695E-02 |
| | 9.353E-03 | 1.396E-02 | 1.518E-02 | -2.252E-02 | 4.269E-01 |
| AR 3: | 1.626E-01 | 1.314E-001 | 1.566E-02 | -3.167E-02 | -3.312E-01 |
| . | 9.621E-02 | 1.163E-01 | 1.038E-01 | -1.219E-02 | -3.433E-01 |
| | 8.128E-03 | 6.785E-02 | 1.390E-01 | 8.892E-02 | -2.844E-01 |
| | -5.933E-03 | -2.143E-03 | 4.915E-02 | 1.769E-01 | 3.041E-02 |
| | -2.750E-03 | -4.317E-03 | -3.087E-03 | 2.124E-02 | 1.486E-01 |
| MA 0: | 2.054E+03 | 0.000E+00 | 0.000E+00 | 0.000E+00 | 0.000E+00 |
| . | 7.004E+01 | 1.748E+03 | 0.000E+00 | 0.000E+00 | 0.000E+00 |
| | 1.541E+01 | 4.795E+01 | 1.416E+03 | 0.000E+00 | 0.000E+00 |
| | 5.248E+00 | 8.766E+00 | 3.001E+01 | 1.027E+03 | 0.000E+00 |
| | 2.040E+00 | 2.304E+00 | 4.085E+00 | 1.285E+01 | 5.473E+02 |
| MA 1: | 1.029E+03 | 2.052E+02 | -2.441E+01 | -6.921E+01 | -2.536E+02 |
| | 2.143E+02 | 7.526E+02 | 1.185E+02 | -5.187E+01 | -2.630E+02 |
| | -3.099E+00 | 1.201E+02 | 6.456E+02 | 6.166E+01 | -2.293E+02 |
| | -2.926E+01 | -2.075E+01 | 6.490E+01 | 5.044E+02 | -2.538E+01 |
| | -1.201E+01 | -1.472E+01 | -1.219E+01 | 1.676E+01 | 1.461E+02 |

Note: $P' = 15$, $\alpha = 0.97$

Table 5. Interpolation model coefficients

| $\beta = 1$: | 0.93356 | -0.14420 | 6.2752E-02 | -2.3873E-02 |
|---|---|---|---|---|
| | 0.22612 | -8.6026E-02 | 3.7436E-02 | -5.7824E-03 |
| $\beta = 2$ | 0.75059 | -0.1940 | 8.6363E-02 | -2.8541E-02 |
| | 0.49518 | -0.1636 | 7.2851E-02 | -1.8829E-02 |
| $\beta = 3$: | 0.49518 | -0.1636 | 7.2851E-02 | -1.8829E-02 |
| | 0.75059 | -0.1940 | 8.6373E-02 | -2.8541E-02 |
| $\beta = 4$: | 0.22612 | -8.6026E-02 | 3.7436E-02 | -5.7824E-03 |
| | 0.03356 | -0.14420 | 6.2752E-02 | -2.3873E-02 |

Note: $\Delta t = 2$ sec and $\delta t = 0.5$ sec. The first line is for causal: $r = 0, -1, -2, -3$, and the second line is for noncausal: $r = 1, 2, 3, 4$

model be $\Delta t$, such that the corresponding Nyquist frequency is a little larger than the frequency beyond which the wind fluctuations has insignificant dynamic effects. Suppose that the time-integration scheme for the solution of the dynamic system requires a much smaller time increment $\delta t$, where $\Delta t/\delta t$ is an integer $S$. It is required to formulate the time series $y[(nS + \beta)\delta t]$ from $y(n \Delta t)$ in which $\beta < S$. There are a number of interpolation methods available (e.g., Oppenheim and Schafer[16]). It is important that the interpolation should not introduce energy at higher a frequency and at the same time be computationally efficient. Recently, new techniques and their applications in various fields have been developed (Li[7]). Their details will be reported elsewhere. Here some concepts relevant to wind engineering are introduced. The interpolation following an ARMA model has to satisfy the following requirement:

Local interpolation: $y[(nS + \beta)\delta t]$ is simulated from $y(m \Delta t)$ with $m = n - Q_I^-, n - Q_I^- + 1, \ldots, n, \ldots, n + Q_I^+$, in which $Q_I^-$ and $Q_I^+$ are small integer numbers. The conventional global interpolation involving the total time series is not suitable for the present application.

Stability: The interpolation is said to be stable if a bounded time series after interpolation still remains bounded.

Accuracy: The spectral density functions represented by $y[(nS + \beta)\delta t]$ are the same as those of $y(n \Delta t)$ when the frequency is less than $1/2\Delta t$, and zeros in the frequency range $1/2\Delta t \sim 1/2\delta t$.

The interpolation techniques may be classified as linear, polynomial or trigonometric. Frequently, a piecewise linear interpolation of the discrete data is utilized. Although this method is the simplest, it may introduce large error in the spectral density function. The polynomial interpolation is the next level of interpolation. For example, Li[7] developed a cubic polynomial interpolation which results in a process continuous at its first-order time derivative and involves three multiplications and additions at each discrete time interval. The trigonometric interpolation utilized by Saunders and Collings[11] and further developed in this study is found to be the most suitable choice for wind engineering applications. In the following a basic concept of the trigonometric interpolation developed in this study is provided.

The discrete time series can be viewed as a process, $y^{\Delta t}(t)$, consisting of numerous pulses:

$$y^{\Delta t}(t) = \sum_{n = -\infty}^{\infty} y(n \Delta t) \Delta t \delta(t - n \Delta t) \qquad (25)$$

in which $\delta(t - n \Delta t)$ is the Dirac delta function. Its Fourier transform is written as

$$Y^{\Delta t}(f) = \int_{-\infty}^{+\infty} \sum_{n = -\infty}^{\infty} y(n \Delta t) \Delta t \delta(t - n \Delta t) \exp(-j2\pi f t) \, dt$$

$$= \sum_{n = -\infty}^{\infty} y(n \Delta t) \exp(-j2\pi f n \Delta t) \Delta t \qquad (26)$$

The preceding equation shows that $Y^{\Delta t}(f)$ is cyclic with the interval $1/\Delta t$, and $Y^{\Delta t}(f) = \overline{Y^{\Delta t}(1/\Delta t - f)}$ in which the overbar represents the conjugate. Similarly, the time series with a time increment $\delta t$ can be viewed as a pulse process $y^{\delta t}(t)$, and the corresponding Fourier transform-

ation becomes

$$Y^{\delta t}(f) = \sum_{m=-\infty}^{\infty} y(m\delta t) \exp(-j2\pi f m\delta t)\delta t \qquad (27)$$

Define a transfer function $H(f)$ which satisfies

$$H(f) = \frac{Y^{\delta t}(f)}{Y^{\Delta t}(f)} \qquad (28)$$

For the ideal case, $H(f) = 1$ for $f < 1/2\Delta t$ and $H(f) = 0$ for $1/2\Delta t < f < 1/2\Delta t$. In the following, a procedure is developed to carry out in the time domain the transformation described in the preceding equation.

The interpolation model developed here is based on the convolution of a finite and infinite wave form. Let the frequency range $-1/2\delta t \sim 1/2\delta t$ be discretized into $SQ^I$ frequency points with the frequency increment $\Delta f = 1/2(2Q/\Delta t)$, in which $2Q^I$ is called the interpolation model order. Within the frequency range $-1/2\Delta t \sim 1/2\Delta t$, $H(f)$ is described as

$$H(m \Delta f) = 1 \qquad \text{for } -Q^I \leqslant m \leqslant Q^I \qquad (29)$$

at the frequency $\pm 1/2\Delta t$, $H(f)$ is equal to 1/2 to account for the transient from 1 to 0:

$$H(m \Delta f) = \tfrac{1}{2} \qquad \text{for } m = \pm (Q^I + 1) \qquad (30)$$

and beyond the frequencies $\pm 1/2\Delta t$, $H(f)$ is given by

$$H(m \Delta f) = 0 \qquad (31)$$
$$\text{for } Q^I + 1 < m \leqslant SQ^I \quad \text{and} \quad -Q^I - 1 > m \geqslant -SQ^I + 1$$

A discrete Fourier transformation of $H(m \Delta f)$ leads to:

$$h(r\delta t) = \sum_{m=-SQ^I+1}^{SQ^I} H(m \Delta f) \exp\left(j\pi \frac{mr}{SQ^I}\right) \Big/ (2SQ^I) \qquad (32)$$

in which $r = 0, 1, 2, \ldots, SQ^I$. If $h(r \Delta t)$ is used as the convolution kernel for interpolation:

$$y^{\delta t}[m\delta t] = \sum_{r=-SQ^I+1}^{SQ^I} h(r\delta t)y^{\Delta t}[(m-r)\delta t] \qquad (33)$$

then taking the discrete inverse Fourier transformation of $h(r\delta t)$ leads to

$$\tilde{H}(f) = \sum_{r=-SQ^I+1}^{SQ^I} h(r\delta t) \exp(-j2\pi fr\delta t) \qquad (34)$$

Obviously, at the frequency $m \Delta f$ with $m$ as an integer number, we have

$$\tilde{H}(m \Delta f) = H(m \Delta f) \qquad (35)$$

and when $f$ is between $[m \Delta f \sim (m+1) \Delta f]$, $\tilde{H}(f)$ exhibits oscillatory signature about the ideal transfer function $H(f)$. However, the oscillations decrease with an increase in the order $Q^I$. As an example, Fig. 9(a) and (b) demonstrate comparisons of an ideal transfer function, with the transfer function given by Saunders and Collings[11], the conventional approach representing truncated trigonometric functions and the present study. It is noted that
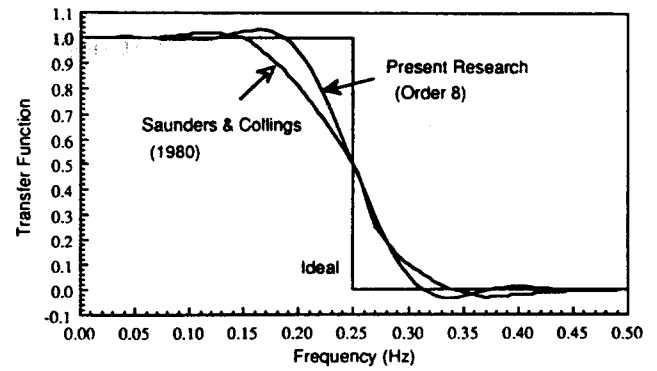


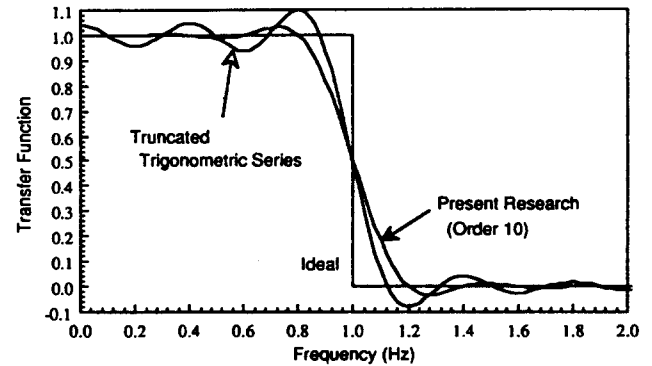*Fig. 9(a).   Transfer functions of interpolation models*



*Fig. 9(b).   Transfer functions of interpolation models*

with the same interpolation model order, the transfer function represented by the interpolation form introduced by the present study is closer to the ideal transfer function. Further improvement is possible by utilizing a higher order filter.

Considering that $y^{\Delta t}(m\delta t) = 0$ for $m\delta t \neq n \Delta t$ in which $n$ is an arbitrary integer number, equation (33) can be rewritten as

$$y^{\delta t \Delta}(Sn + \beta)\delta t] = \sum_{r=-Q^I+1}^{Q^I} h_{\beta r} y^{\Delta t}[(n+r) \Delta t]/S \qquad (36)$$

in which $h_{\beta r}$ is a rearrangement of $h(r\delta t)$. Virtually the interpolation is carried out at each time interval $(Sn + \beta)\delta t$ by $2Q^I$ multiplications and additions,

$$y[(Sn + \beta)\delta t] = \sum_{r=-Q^I+1}^{Q^I} h_{\beta r} y[(n+r) \Delta t] \qquad (37)$$

An example of this interpolation model is considered here. A fluctuating component of wind velocity according to the Davenport spectrum is simulated by an ARMA model with $\Delta t = 2$ sec, and is further interpolated to form the wind velocity with $\delta t = 0.5$ sec. This interpolation is performed by the above described interpolation model of order 8 (Table 5). In order to validate the interpolation model, the discrete time series before interpolation is taken from a continuous time function instead of an ARMA model. In Fig. 10, the continuous time function and the discrete time series before and after the interpolation are plotted. It is noted in this figure that the continuous function and the time series simulated by interpolation are almost coincident.
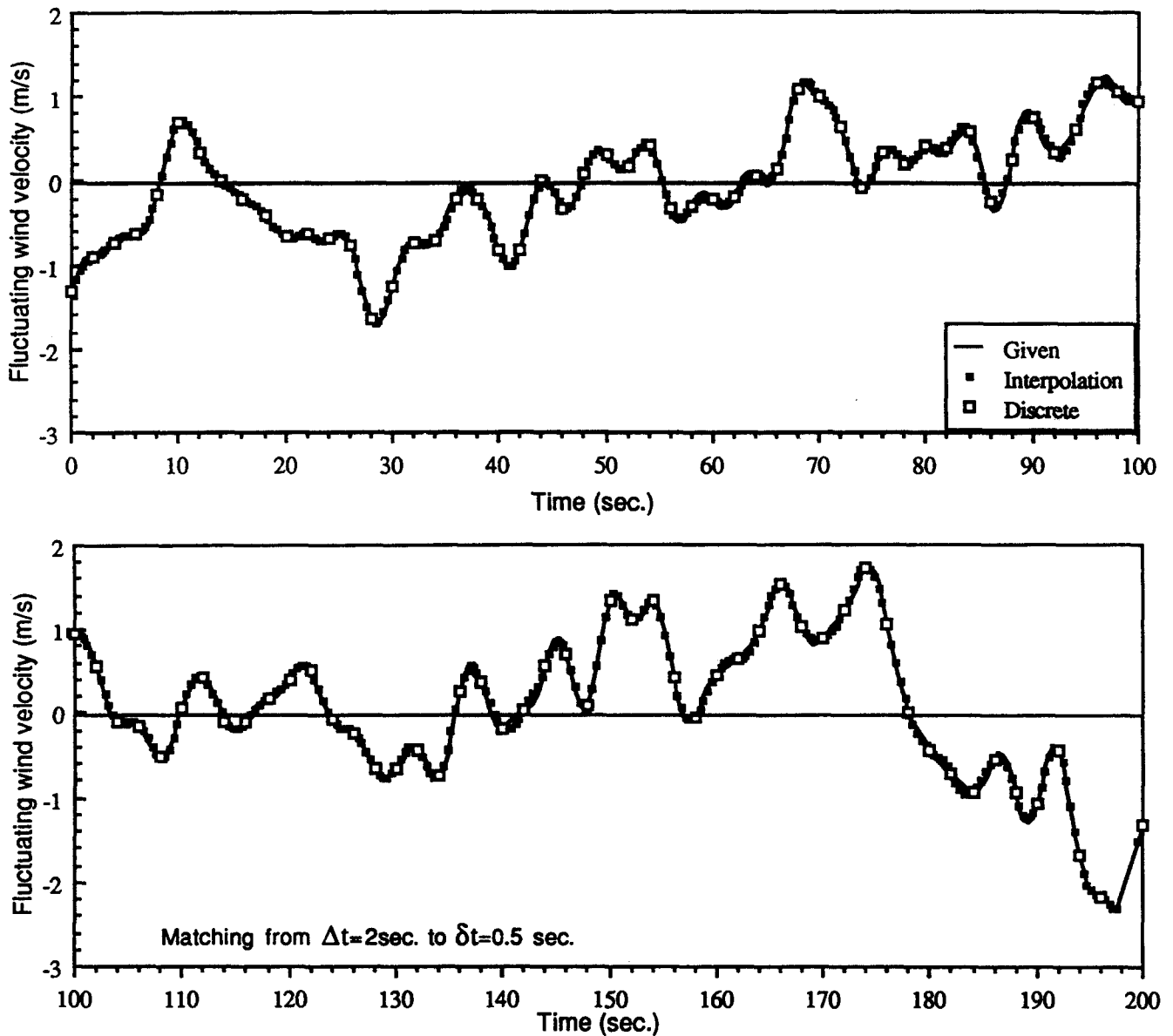
*Fig. 10.    Continuous, discrete and interpolated wind velocities*

## CONCLUDING REMARKS

The simulation of wind velocity and wind force fields can be performed by ARMA models. The ARMA representation of such processes is possible by a number of matching procedures of which the two-stage-matching procedures is most widely used. However, the nature of the dynamic systems and the numerical schemes utilized for solving the dynamic response often require a small time increment, which renders a straightforward application of ARMA models difficult.

A three-stage-matching method is developed in which a multivariate ARMA model utilizing small time increments can be matched to a target wind spectrum. A salient feature of this method is that despite the low order of the model the simulated and target spectral density functions are in good agreement for typical wind engineering applications involving wind sensitive structures. A more general technique utilizing the interpolation approach is presented. First, the time series is generated from an ARMA model with relatively widely spaced time increments selected according to the maximum frequency of interest. Then, by using the interpolation technique

intermediate values at desired time increments are obtained. The interpolation procedure must ensure that the interpolation does not introduce significant spectral contents of high frequency. In this research a digital filter utilizing trigonometric interpolation is developed based on a discrete convolution of finite and infinite waveforms. The two-stage-approach involving the generation of time series by the ARMA model at a convenient time increment and a subsequent interpolation to a desired time increment offers a computationally efficient simulation scheme for processes which otherwise pose difficulty in utilizing straightforward ARMA models.

## ACKNOWLEDGEMENT

## REFERENCES

1    Box, G. E. P. and Jenkins, G. M. *Time Series Analysis: Forecasting and Control*, Holden–Day, San Francisco, California, 1970
2    Davenport, A. G. 'The spectrum of horizontal gustiness near the ground in high winds, *Q. J. Roy. Met. Soc.*, 1961, **87**, 194–211
3    Harris, R. I. On the spectrum and auto-correlation function of gustiness in high winds, *ERA Report 5273*, 1968
4    Kareem, A. and Dalton, C. Dynamic effects of wind on tension leg platforms, OTC 4229, *Proceedings of Offshore Technology Conference*, Houston, TX, 1982
5    Kareem, A. Wind-induced response analysis of tension leg platforms, *Journal of Structural Engineering*, ASCE, 1985, **111**, 37–55
6    Kareem, A. Wind effects on structures: a probabilistic viewpoint, *Probabilistic Engineering Mechanics*, 1987, **2**(4), 166–194
7    Li, Y. Stochastic response of a tension leg platform to wind and wave fields, Ph.D. Thesis, Department of Mechanical Engineering, University of Houston, 1988
8    Reed, D. A. and Scanlan, R. H. Time series analysis of cooling tower wind loading, *Journal of Structural Engineering*, ASCE, 1983, **109**(2), 538–554
9    Reed, D. A. and Scanlan, R. H. Autoregressive representation of longitudinal lateral, and vertical turbulence spectra, *Journal of Wind Engineering and Industrial Aerodynamics*, 1984, **17**, 199–214
10   Samaras, E., Shinozuka, M. and Tsurui, A. ARMA representation of random process, *Journal of Engineering Mechanics*, ASCE, 1984, **111**, 449–461
11   Saunders, L. R. and Collings, G. Efficient solution of model equations with arbitrary loadings, *Eng. Struct.*, 1980, **2**, 35–48
12   Simiu, E. and Scanlan, R. H. *Wind Effects on Structures*, Second Edition, John Wiley & Sons, New York, NY, 1986
13   Spanos, P. D. and Schultz, K. P. Two-stage order-of-magnitude matching for the Van Karman turbulence spectrum, *4th International Conference on Structural Safety and Reliability*, 1985, I-211–217
14   Spanos, P. D. and Mignolet, M. P. Recursive simulation of stationary multivariate random processes – Part II, *Journal of Applied Mechanics*, 1987, **54**, 681–686
15   Spanos, P. D. and Mignolet, M. P. MA to ARMA modeling of wind, *Proceedings of the 6th U.S. National Conference on Wind Engineering* (A. Kareem, editor), 1989
16   Oppenheim, A. V. and Schafer, R. W. *Digital Signal Processing*, Prentice-Hall, Englewood Cliffs, New Jersey, 1975

## APPENDIX A: WIND SPECTRA

For the sake of completeness the two commonly used wind spectral distributions discussed in this paper are given here. Further details can be found among others, in Davenport[2], Harris[3] and Simiu and Scanlan[12].

The wind spectrum due to Davenport[2] is given by

$$\frac{fG_u(f)}{\kappa U_{10}^2} = \frac{4\chi^2}{(2+\chi^2)^{4/3}} \qquad (A.1)$$

in which $\chi = fL/U_{10}$ and $L$ is the length scale equal to 1200 m. The Harris spectrum is described by

$$\frac{fG_u(f)}{\kappa U_{10}^2} = \frac{4\chi^2}{(2+\chi^2)^{5/6}}$$

in which $\chi = fL/U_{10}$ and $L = 1800$ meters.